Supplementary Information

Skin-inspired self-healing semiconductive touch panel based on novel transparent stretchable hydrogels

Xingkui Guo,[a] Fan Yang,*[a] Wenbo Liu,[a] Chuang Han,[a] Yujiao Bai,[a] Xiaolu Sun,[a] Lifeng Hao,[a] Weicheng Jiao [a] and Rongguo Wang*[ab]

[a] National Key Laboratory of Science and Technology on Advanced Composites in Special Environments
Harbin Institute of Technology
Harbin 150080, P. R. China

[b] Shenzhen STRONG Advanced Materials Research Institute Co., Ltd
Shenzhen, P. R. China

E-mail: wrg@hit.edu.cn; yngfan01@163.com

Materials and methods

Materials. N,N-dimethylacrylamide (DMAA, Analytical Reagent) was purchased from Tokyo Chemical Industry Co. Initiator potassium peroxydisulfate (KPS, Analytical Reagent), N,N,N′,N′-tetramethylethylenediamine (TEMED, Analytical Reagent) and Conductive ink (Particle size $\leq 3\mu$m) were obtained from Sigma-Aldrich Co. TiO_2 nanosol (anatase; 15% in wt.%) was provided from Hangzhou Wanjing New Material Reagent Co. The average size of TiO_2 nanoparticles was around 15 nm. Dielectric elastomer Very High Bond (VHB) 4905/4910 was supplied by 3M Co. TiO_2 nanosol was purified to 20 wt.%. KPS was recrystallized before use. Other reagents were used as-received without any further purification or analysis.

Preparation of nanocomposite hydrogel. In a typical procedure, firstly, the nanocomposite hydrogel was synthesized by mixing DMAA monomer (molar concentration was 1.17 M) in deionized water. The initiator KPS 3.36 wt.%, with respect to the DMAA monomer, were added and stirred for 5 min. Subsequently, TEMED 1.36 wt.%, with respect to the weight of the DMAA monomer, was added and stirred for 40s. Secondly, the different TiO_2 nanoparticle loadings, namely TiO_2-0/PDMAA (0 wt.% TiO_2 of the DMAA monomer), TiO_2-35/PDMAA (35 wt.% of the DMAA monomer), TiO_2-70/PDMAA (70 wt.% of the DMAA monomer), TiO_2-110/PDMAA (110 wt.% of the DMAA monomer), were added as the cross-linker. All preparation processes of the nanocomposite hydrogels were performed inside a nitrogen-filled glove box with O_2 and H_2O below 300 ppm. The solutions were poured into polymethylmethacrylate (PMMA) molds with different types such as strip, circular

and rectangular, for touch panel. The hydrogel was prepared after several hours at 50 °C. The preparation and curing process is schematically shown in Figure 1.

A semiconductive touch strip. The gel strip was constructed in order to verify the 1D semiconductive touch sensing system. The semiconductive gel strip was prepared with nanocomposite hydrogel containing 70 wt.% TiO_2 nanoparticles and electrodes (Pt wires). Each side of the touch strip was installed an electrode and connected a current meter. Then, both sides of the strip were applied the same phase of alternating current (AC) power (17 kHz, $\pm$ 0.6V).

To verify the relation between the finger-corner distance touching current, a 1D gel strip, 100 mm in length, was constructed. The touching current induced by a finger at various touch positions, η, was recorded in Figure 3d. In addition, the gel strip was stretched (λ=2), and various positions were touched, similar to the preceding undeformed state (Figure 3e). During the experiments, the touch strip was washed with deionized water to remove impurities.

A semiconductive touch panel. The type of the semiconductive touch panel depended on the experimental purpose. The circular and rectangular types were prepared for the biaxial stretching situation, and 2D demonstration and comparison with the simulation, respectively. The semiconductive touch panel and touch strip were the same TiO_2 loading (70 wt.%) and thickness (3 mm). When the panel was first operated after connected to computer through the CB, the output figure could not be represented well (too small or too large). The calibration tool of the controller board was utilized through conducting a four-point calibration for optimal accuracy.

Epidermal touch panel. Epidermal touch panel was designed using the VHB (3M, a type of adhesive tape) as the dielectronic material. The panel connected to four electrodes at each corner and fixed on the VHB film. The epidermal touch panel could be mounted to human skin and can still be operated as an input device without sacrificing its functionalities. The panel after the attachment was transparent and still can accurately and fast detect various motions, including swiping, dragging, holding and tapping.

Characterization. The morphology of freeze-dried TiO_2/PDMAA nanocomposite hydrogel was characterized taking Scanning electron microscopy (SEM) on a Zeiss Supra 55 microscope (Carl Zeiss AG, Germany). Transmission electron microscopy (TEM) image and selected area electron diffraction (SAED) were acquired on a JEOL JEM2011 microscope at 200 kV. For TEM sample preparation, a small amount of hydrogel deposited on the copper grid was freeze-dried before observation. X-ray diffraction (XRD) data were recorded on Empyrean diffractometer (Panalytical Co. Dutch) with Ni-filtered Cu Kα radiation (40 kV, 40 mA). Attenuated total reflectance-Fourier transform infrared (ATR-FTIR) was carried out on a Nicolet IS50 spectrometer (Thermo fisher Scientific Co. USA) with a diamond ATR crystal as the window material. The thermal stability of the nanocomposite hydrogel was characterized by using thermal gravimetric analysis (TGA, Mettler Toledo Co. Swiss Confederation) from 25 to 800 ºC with a heating rate of 10 K/min under N_2 flow. The rheological behavior of the nanocomposite hydrogel was investigated by using AR 2000ex rheometer (TA Instruments Co. UK). Dynamic frequency sweep was measured from

0.1 to 420 Hz at 25 ºC in the oscillation mode with a fixed oscillatory strain of 1%. The optical transmittances of nanocomposite hydrogels containing TiO_2 nanoparticles were investigated using UV-VIS spectroscopy (Lambda-950, PerkinElmer) with an acrylic cuvette in a range of visible light (380-780 nm). An acrylic cuvette with deionized water was used as a reference. The photocurrent characterization of nanocomposite hydrogels was conducted by an electrochemical workstation (Autolab, Metrohm Co.). A 300 W xenon lamp was selected as the light source and the test methods were according to the Zhu et al.[1] The samples of all of self-healing characterizations were the nanocomposite hydrogel containing 70 wt.% TiO_2 nanoparticles.

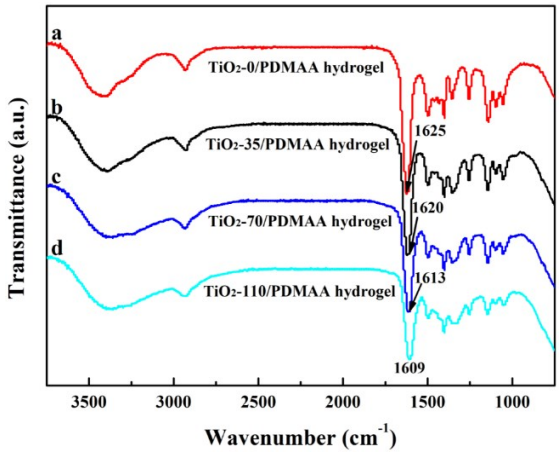

Figure S1. FTIR spectra a) PDMAA hydrogel; and TiO_2/PDMAA nanocomposite hydrogel prepared with the amount of b) 35, c) 70, d) 110 wt.% TiO_2.

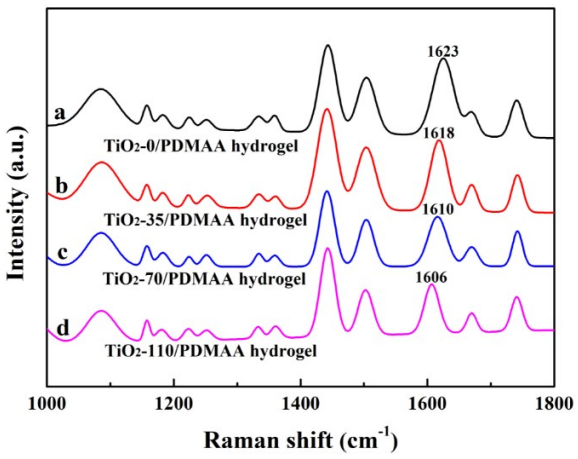

Figure S2. Raman spectra a) PDMAA hydrogel; and TiO_2/PDMAA nanocomposite hydrogel prepared with the amount of b) 35, c) 70, d) 110 wt.% TiO_2.

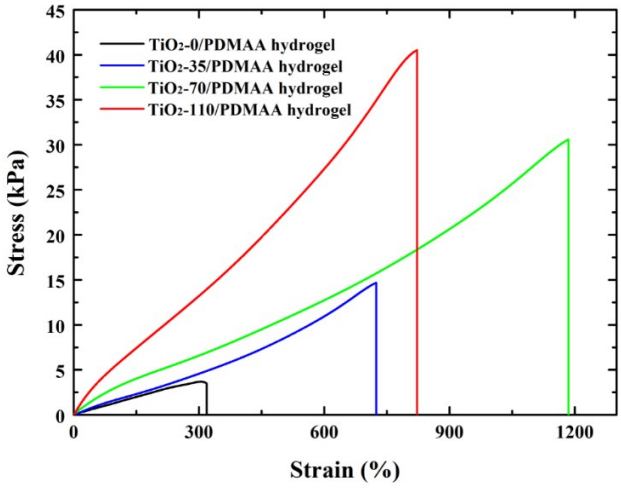

Figure S3. The tensile measurements of nanocomposite hydrogels with different TiO_2 weight ratios.

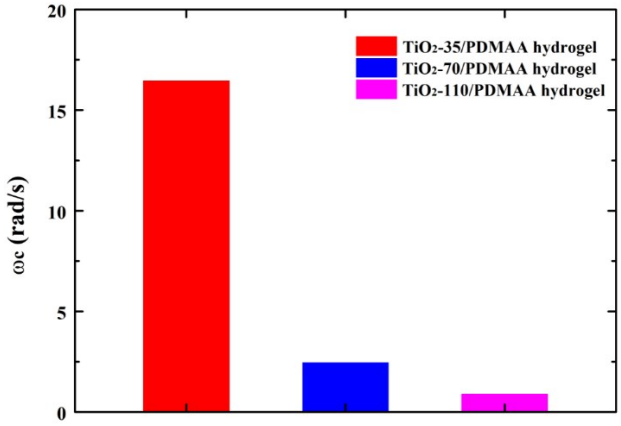

Figure S4. The crossover frequency (ω_c) obtained from frequency sweeps for hydrogels with different TiO_2 loadings. The representative crossover frequencies, where the storage modulus G′ (elastic modulus) was equal the loss modulus G″ (viscous modulus), in Figure 1c were denoted using arrows.

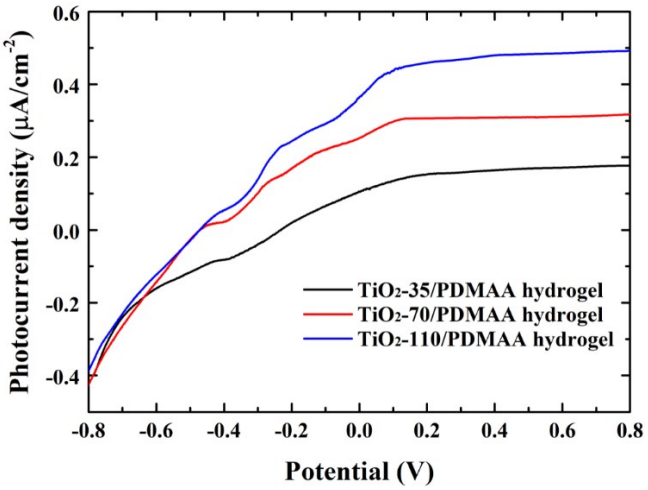

Figure S5. Variation of photocurrent density vs. applied potential of photoelectrodes.

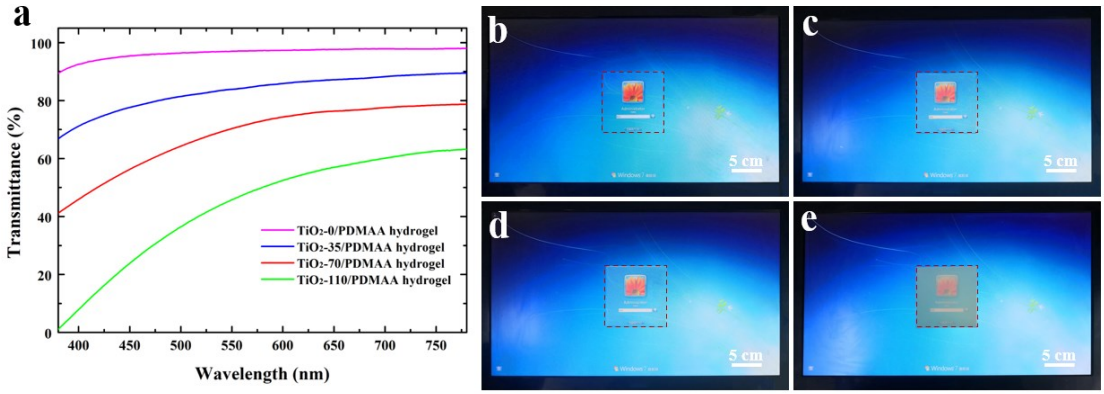

Figure S6. a) Transmittances of light through the nanocomposite hydrogels. Nanocomposite hydrogel was attached on the computer screen with a loading of b) 0, c) 35, d) 70, e) 110 wt.% TiO_2. The gels with 0 wt.%, 35 wt.% 70 wt.% and 110 wt.% TiO_2 concentrations showed 95.91 %, 84.84 %, 70.17 % and 37.86 % average transmittance for the range of visible light, respectively.

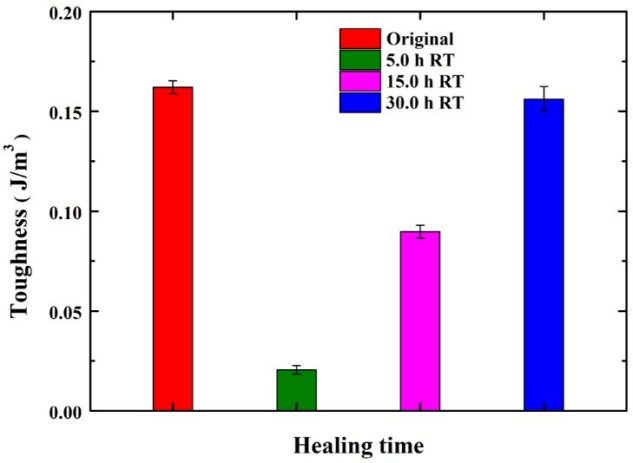

Figure S7. Mechanical healing efficiencies for different healing time; RT: Room Temperature. The toughness is used to quantify the mechanical healing efficiencies, because this takes into account the restoration of both stress and strain (area under the stress-strain curve).

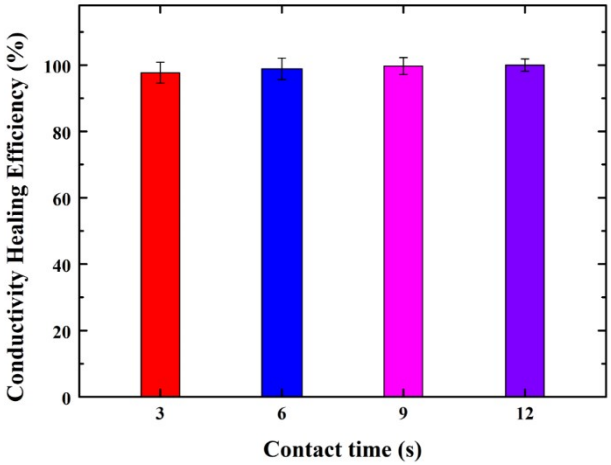

Figure S8. Conductive healing efficiencies vs. contact time. The conductive healing efficiency term, as the proportion of conductivity restored relative to the original conductivity.

Sensing mechanism of the 1D touch strip. To investigate the 1D sensing mechanism of a semiconductive touch panel, a 1D strip model was designed which consists of two resistors and three capacitors (Figure S13).

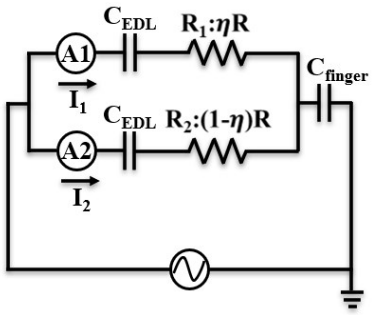

Figure S9. The electrical circuit diagram of the 1D semiconductive touch strip.

When the semiconductive touch strip was touched by a finger, current was generated between the electrode and the finger position. The magnitudes of the two resistors were depended on the touch location.

$$R_1 = \eta R \tag{S1}$$

$$R_2 = (1-\eta)R \tag{S2}$$

where R and η represent the total resistance and a normalized position, respectively. Because each resistive part was connected with a C_{EDL} in series, the impedance (Z) of two pathways can be represented as

$$Z_1 = R_1 - \frac{\varphi}{2\pi\nu C_{EDL}} \tag{S3}$$

$$Z_2 = R_2 - \frac{\varphi}{2\pi\nu C_{EDL}} \tag{S4}$$

The testing frequency and the area of the double layer were approximately 17 kHz and 10^{-5} m^2, respectively, and the capacitance per unit area of C_{EDL} was on the order of 0.1 F/m^2.[2] Therefore, the reactance of the double layer was $-\varphi\frac{1}{2\pi\nu C_{EDL}} \approx -9\varphi$. In addition, the resistance of the semiconductive touch strip ($R \approx 1000\Omega$) was larger than the reactance of the gel strip, so the resistance was approximate to the impedance ($Z \approx R$). The approximation led to the touching current could be calculated by a ratio between two resistances. When a coupling capacitance formed in finger/hydrogel interface (

C_{finger}) was added to the circuit in series, the total current (I_T) flowing through the circuit was

$$I_T = \frac{U}{\frac{R_1 R_2}{R_1 + R_2} - \frac{\varphi}{2\pi v C_{finger}}} \tag{S5}$$

$$I_1 \approx I_T \cdot \frac{R_2}{R_1 + R_2} = (1 - \eta) I_T \tag{S6}$$

$$I_2 \approx I_T \cdot \frac{R_1}{R_1 + R_2} = \eta I_T \tag{S7}$$

In addition, Formula S5 and S6 were rearranged into

$$(1 - \eta) = \frac{I_1}{I_T} \tag{S8}$$

$$\eta = \frac{I_2}{I_T} \tag{S9}$$

Parasitic capacitance and baseline current. The panel in a steady or untouched state shouldn't theoretically generated the electrical potential difference, so the panel should be no current flow. Whereas current (namely baseline current) was incurred in the steady state owing to parasitic capacitance that is usually formed between a circuit and environments.[3] As shown in Figure S14, the baseline current was determined by the parasitic capacitance that usually existed between environments and the panel in the semiconductive touch panel system, which is regarded as a noise signal. Thus, the performance of the semiconductive touch panel can be improved through reducing the baseline current. As shown in Figure 3c, 3d and 5a-d, various methods such as changing the thickness, surface area and resistance could be conducted to reduce the parasitic capacitance of the panel. Meanwhile, it should be noted that the semiconductive touch

panel has a lower baseline current than the ionic touch panel in the hydrogel system.

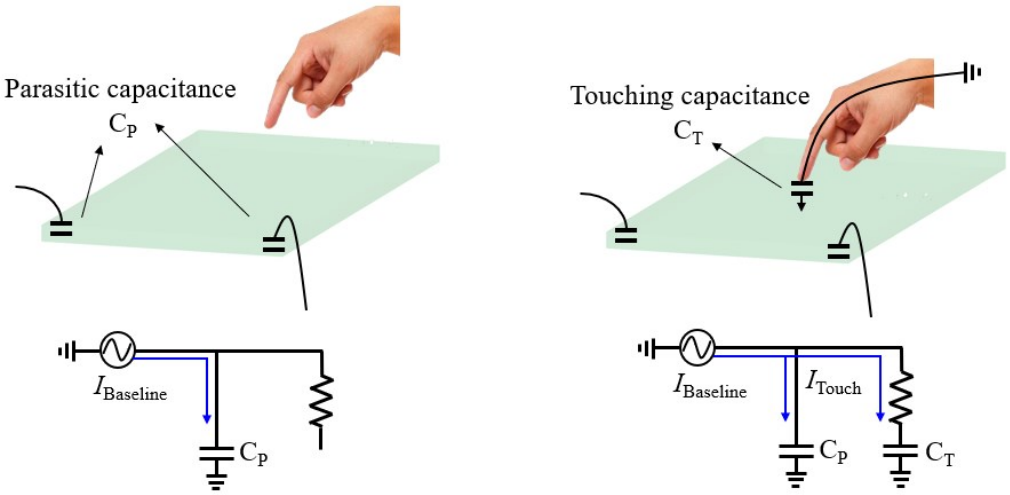

Figure S10. Schematic representation of the parasitic capacitance and current flow in a capacitive touch panel and the corresponded electrical circuit diagrams.

Latency of the semiconductive touch panel. A touching current induced at the moment of touching was analyzed to investigate the latency of the semiconductive touch panel. A digital multimeter (Keysight 34410A, maximum scan rate of 50 samples per second) was used to measure the current. As shown in Figure S15, the current signal was detected without any delays. Therefore, we supposed that the response time of the touch strip may be less than 20 ms.

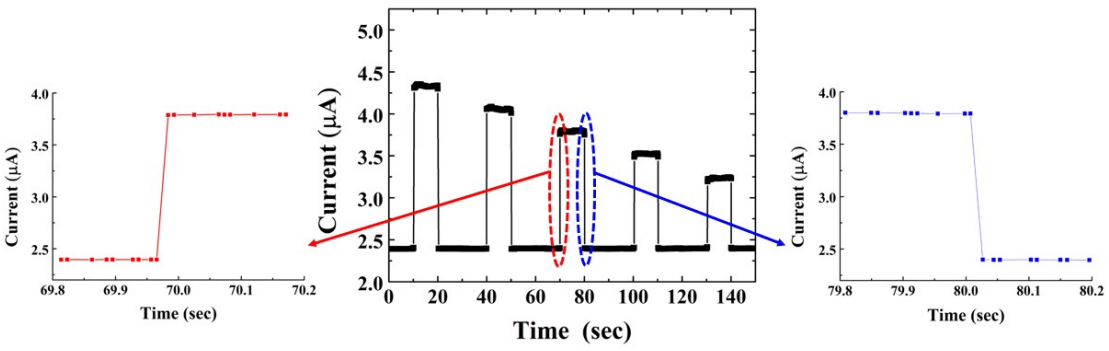

Figure S11. The response time of a touching current was analyzed to investigate the latency of the semiconductive touch panel. The graphs were magnified for determining the response time of a touching current.

The effect of the thickness of a touch panel on the response time of the touch panel was investigated. The resistance was determined by the thickness, the thicker panel corresponded to the smaller of the resistance. High resistance causes an increase in the RC delay ($T_\tau = RC$) of circuit. Therefore, an appropriate thickness of the panel was significant for obtaining optimal user experience. As shown in Figure S16, the latency of a touch strip with various thicknesses (0.5 mm, 1 mm, 2 mm and 3 mm) was studied. However, we could not detect any delays in the semiconductive touch strip system, even the highest resistance among them (a 0.5 mm thick touch strip). Instead, the RC delay of the touch strip could be calculated by the electrical theory. The resistance of the 0.5 mm thick gel was ~9 k Ω, and the capacitance of the finger is ~100 pF.[4] Thus, the RC delay in the touch strip was approximately 9×10^{-5} s, which was much smaller than the minimum interval of sampling in our current meter.

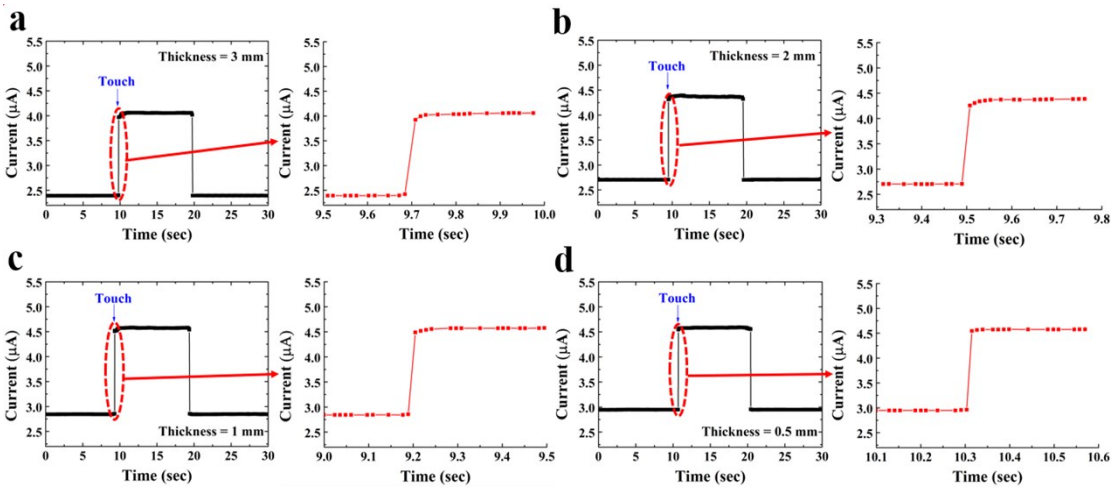

Figure S12. A touch strip with different thicknesses of a) 3 mm, b) 2 mm, c) 1 mm and d) 0.5 mm were investigated for the response time.

Accumulated touching currents of a hydrogel strip during the stretching. A hydrogel strip (100 × 15 × 3 mm) was uniaxially stretched with a strain rate of 0.25/min

and touched by a finger during the period of stretching as shown in Figure S17. The currents were incurred by the touch and stretch simultaneously, but the effect of the two factors on the current signal were different. Both baseline current and touching current showed a slope in the current signal during the stretching period of the strip, whereas the slope of the baseline current was much smaller than the touching current. Therefore, we can distinguish the current signals through comparing the slope of the current. In addition, the same phenomenon can be observed when the hydrogel panel was equi-biaxially stretched. Thus, with the uniaxial stretch, the slope of the current could be exploited to distinguish each current signal from stretching and touching.

Furthermore, we supposed that the enlargement of the baseline current because of its increased parasitic capacitance caused probably by an expansion of the surface area of the hydrogel. When the hydrogel strip was uniaxially stretched, the surface area of the gel can be represented by the following formulas

$$\begin{aligned}\frac{S}{S_0} &= \frac{H_xH_y + H_xH_z + H_yH_z}{L_xL_y + L_xL_z + L_yL_z} \\ &= \frac{L_xL_y\sqrt{\lambda_x} + L_xL_z\sqrt{\lambda_x} + L_yL_z/\lambda_x}{L_xL_y + L_xL_z + L_yL_z}\end{aligned} \tag{S10}$$

where S_0 and S represent the surface areas of the hydrogel strip under the original and stretched state, respectively. L, H and λ are the initial length, current length and the stretch of the hydrogel, respectively. The subscripts L, H and λ represented a direction of the coordinate axis. The materials were assumed to possess incompressibility, $\lambda_x\lambda_y\lambda_z = 1$, and a condition of uniaxial stretch, $\lambda_y = \lambda_z = \frac{1}{\sqrt{\lambda_x}}$, was applied. When the length (L_x), width (L_y) and thickness (L_z) of the hydrogel strip were 100 mm, 15 mm

and 3 mm, respectively. We typically obtained $S/S_0 = \left(1800\sqrt{\lambda_x} + \frac{45}{\lambda_x}\right)/1845$. As shown in Figure S17, the surface area of gel increased as it was stretched, and the increase was compared with the experimentally measured currents. The change of surface area and the baseline current showed a similar tendency. In addition, the similarity of baseline current and the change in surficial area of the semiconductive touch panel was better than the ionic touch panel from the experiment results.

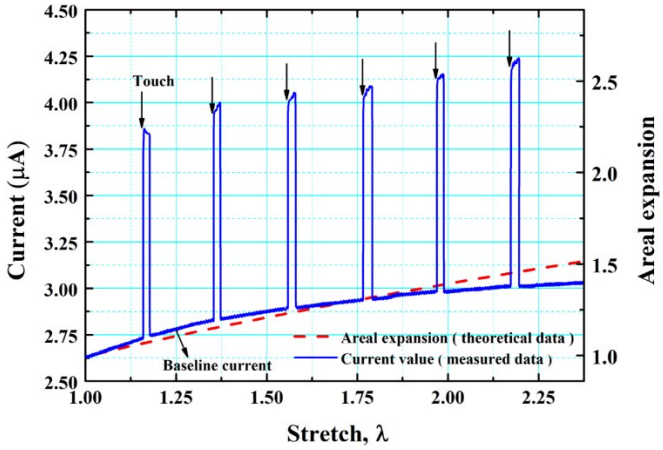

Figure. S13. Accumulated touching currents during a hydrogel strip (100 × 15 × 3 mm) was uniaxially stretched with a strain rate of 0.25/min.

Strain rate effects of a gel strip during a uniaxial stretching. We investigated the effect of changing strain rate on the current signals from a gel strip for use in dynamic applications. As shown in Figure S18, Various strain rate such as 0.25/min, 0.5/min, 0.75/min and 1/min were conducting, as a result, the baseline current showed insensitivity to strain rate in the range of 0.25-1/min.

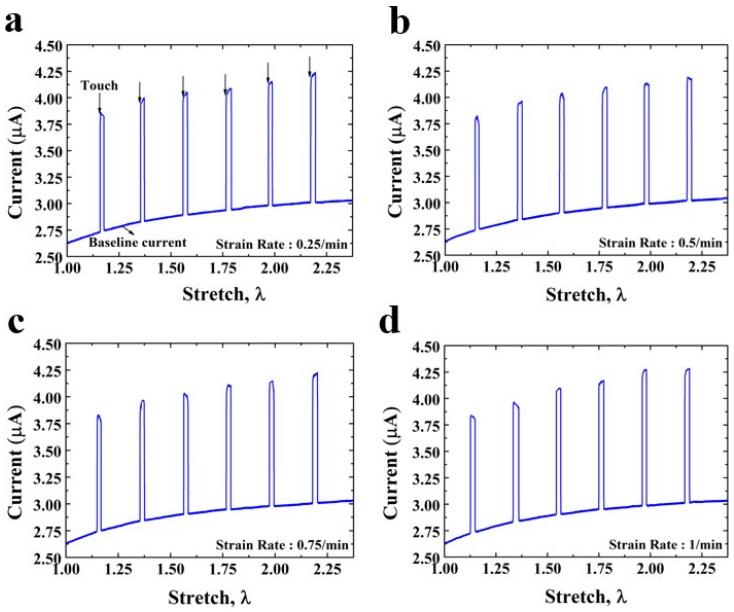

Figure S14. The effect of strain rate (0.25, 0.5, 0.75 and 1/min) on the gel strip during a uniaxial stretch. The strain rate made no difference to the baseline currents during stretching.

Resolution of the semiconductive touch panel. High resolution is a crucial factor for designing an accurate and reliable touch panel. The capacitive touch sensing systems, projected capacitive touch and surface capacitive touch, had higher resolution among the touch sensing systems, including surface acoustic wave touch, bend wave touch and optical touch and capacitive touch. The surface capacitive touch was adopted in our semiconductive touch panel because the projected capacitive touch was typically used for smartphones. The projected capacitive touch panel consisting of a grid pattern of ITO, and the change in the mutual capacitance of grids was measured for confirming the touch position. Furthermore, the resolution of the projected capacitive touch was determined by the grid interval and the number of grids. However, the surface capacitive touch panel had only one layer of continuous conductive material and without any grids. If the material of touch panel is homogeneous, the resolution of the

surface capacitive touch panel will be limited by the resolution of the current meter. The current meter using in our measurement possessed a nanoampere-range resolution, and the touch strip showed a resolution on the order of 10^{-4} m correspondingly. A hydrogel strip was swiped by a finger from A1 to A2 (Figure S19a), and the current was continuously recorded through exploiting the A1 current meter during the swiping. As shown in Figure S19b, the current signals were linearly decreased as the increment of the distance between the touch position and the electrode A1. We observed that on the order of 10 touch positions were perceived within 1 mm of swiping through the magnified view of the current graph (Figure S19c), which correspond to a 10^{-4} m resolution.

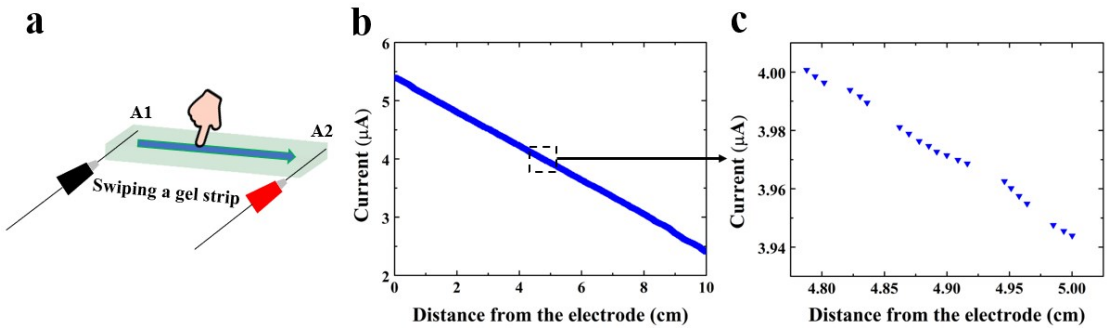

Figure S15. a) A finger swiped on the hydrogel strip from electrode A1 to electrode A2. The current was detected in real time by a current meter connected to the electrode A1during the swiping. b) The current decreased linearly as the increment of the distance between the touch position and the electrode A1. c) The current graph was magnified.

Stability of the semiconductive touch panel. The experimental apparatus for repeatedly touching the 2D panel was designed to investigate the stability of the touching current as shown in Figure S21a. A dielectric material, a 1-mm-thick polymethylmethacrylate (PMMA) plate, was applied in order to realize electrical

insulation between the gel panel and the printed paper. The same position (0.5, 0.5) of the 2D touch panel was repeatedly touched more than 500 times by a prosthetic finger connected to an external resistance that grounded. The part of touching current was selected and plotted against time as shown in Figure S21b, and the results showed the touching current of the same position was repeatable and stable.

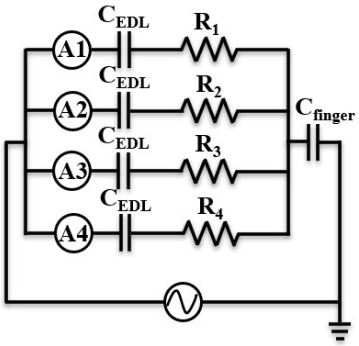

Figure S16. A corresponding electrical circuit diagram of the semiconductive touch panel.

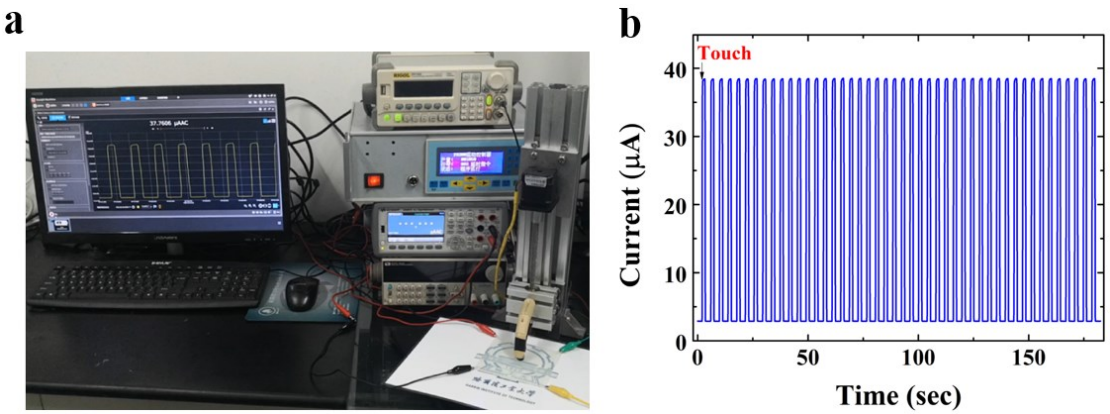

Figure S17. a) The schematic of the same position (0.5, 0.5) of the 2D semiconductive touch panel was repeatedly touched more than 500 times by a prosthetic finger connected to an external resistance that grounded. b) When the 2D touch panel was repeatedly touched by the prosthetic finger, touching current will repeatedly be generated and plotted against time.

The controller board (CB) between the semiconductive touch panel and a

computer. A controller board (CB) was constructed to help communication between a computer and the 2D panel (Figure S22). A drive voltage signal that generated by the CB was applied to each corner of the panel, and the currents to the corners were measured by the CB at the same time. Due to the currents were approximately a few microamperes, the real-time currents were amplified and converted to digital signals by the CB to synchronously calculate coordinates of the finger position.

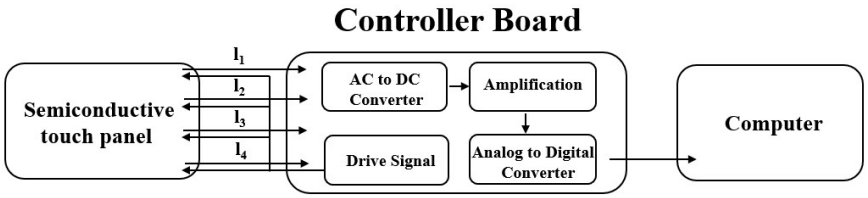

Figure S18. A block diagram of a controller board was constructed to help communication between a computer and the semiconductive touch panel.

The insulation of the epidermal touch panel. To verify the correlation between the thickness of the insulating layer and the leakage current, an experiment was designed and conducted. An additional leakage current was induced after the attachment, which caused a decrease in the touching current and an increase in the baseline current. These results led to the sensitivity of the epidermal touch panel was weakened. As shown in Figure S23, the thickness of the dielectric insulating layer, the VHB (1 mm thick), was increased from 1 mm to 8 mm in 1 mm increment. As a result, the sufficient insulation could strengthen the touch sensitivity of the epidermal touch panel.

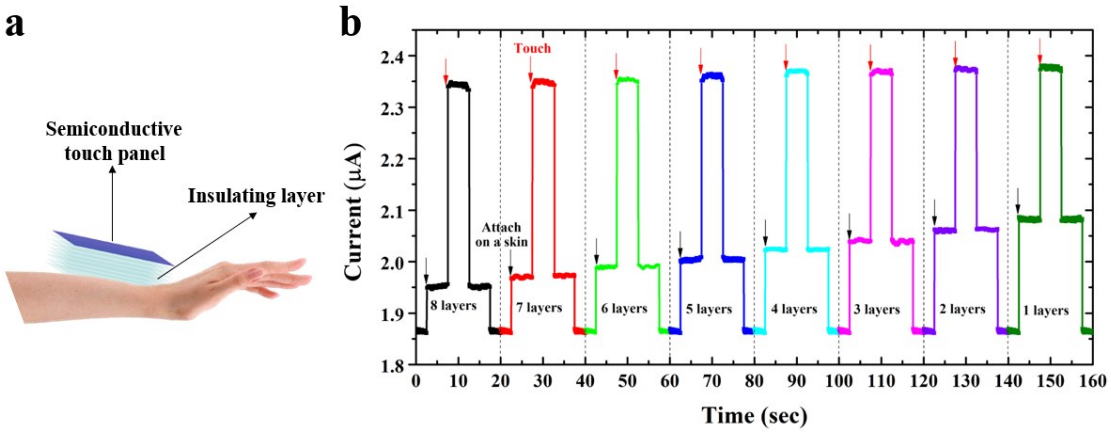

Figure S19. a) The schematic of semiconductive touch panel attached on human skin with different insulating layers. b) The current was measured with different numbers of insulating layer. The thicker insulating layer was more sensitive to touch signals for the semiconductive touch panel.

Resistance of the semiconductive touch panel with various concentrations. Nanocomposite hydrogels (100 mm × 15 mm × 3 mm) containing 1, 5, 10, 20, 40, 70 and 110 wt.% TiO_2 nanoparticles were prepared. The hydrogel follows the resistivity law because it is a resistor:

$$R = \rho\frac{L}{S}$$

Where L and S are the length and the cross-sectional area of the hydrogel strip, respectively. In the hydrogel system, ρ can be substituted by c/W, where c is a constant value, and W is the weight concentration of TiO_2 solution. The resistance can be approximately rewritten as $R = cL/SW$. As shown in Figure S24a, the resistances of hydrogels were measured and showed an inversely proportional relationship with the weight concentration.

As shown in Figure S24b, the baseline currents and the touching currents were measured as a function of the weight concentration. As a result, the baseline current

was influenced by the weight concentration, with the weight concentration increased, the baseline current decreased. Whereas the touching current was insensitivity to the weight concentration.

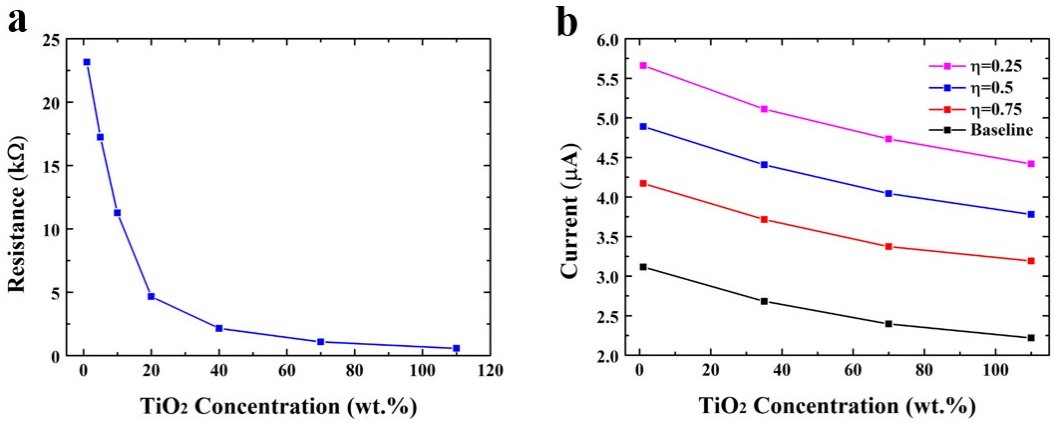

Figure S20. a) Resistance of the semiconductive touch panel with various concentrations of TiO_2 nanoparticles. b) The baseline current and touching current at various η were plotted with different concentrations.

Volatility of semiconductive touch panel. Volatility is a significant factor in a hydrogel owing to water evaporation in the hydrogel. To keep the moisture in the hydrogel, one simple and effective approaches was incorporating different percentage of hygroscopic nanoparticles such as TiO_2 nanoparticles[5]. Thus, the semiconductive touch panel was developed with TiO_2 nanoparticles as a charge carrier. As shown in Figure S25a, the volatility of the nanocomposite hydrogels with different TiO_2 concentrations was investigated. As a result, the performance of maintaining the moisture was enhanced as the increment of the TiO_2 weight concentration. In addition, three hydrogel samples containing TiO_2 nanoparticles, SiO_2 nanoparticles, and pure water were also prepared to check the volatility of the gel (Figure S25b). The test sample was a 3-mm-thick circular shape of 4 cm in diameter, and the volatility of the

hydrogel was evaluated through the ratio ($^{W}/_{W_0}$), where W_0, W were an initial weight and the final weights after evaporation in a vacuum desiccator, respectively. As shown in Figure S25b, the hydrogel containing TiO_2 nanoparticles showed the best performance in terms of maintaining the moisture among the three samples.

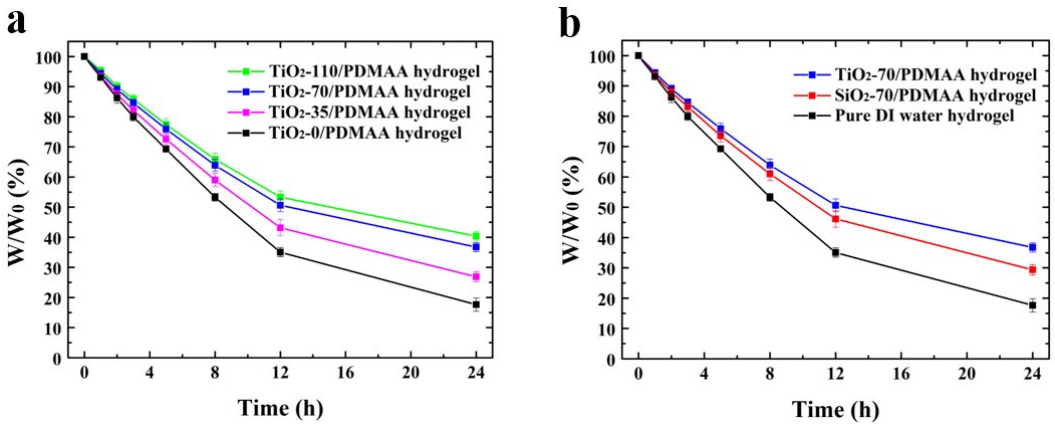

Figure S21. a) Volatility tests of hydrogels containing different TiO_2 loadings. b) Volatility tests of hydrogels containing TiO_2, SiO_2 nanoparticles.

Movie S1

The electrical healing process for the nanocomposite hydrogel with an LED in series with a self-healing electrical conductor.

Movie S2

The diameter of a circular semiconductive touch panel was from 60 mm to 220 mm by being stretched equi-biaxially, which corresponded to more than 1100% of the areal strain. The panel could be operated as an input device without sacrificing its functionalities in a highly stretched state.

Movie S3

Touch repeatedly the same position of semiconductive touch panel by a prosthetic finger connected with an external resistance that grounded. The touching

current was stable.

Movie S4 and S5

An epidermal touch panel could perceive an arbitrary motion of touching, and it was used to write a word.

Movie S6

Chess was played using the epidermal touch panel. Selecting and moving a pawn could be accomplished through a “tapping” gesture.

Movie S7

Angry Birds was played using the epidermal touch panel. Various motions, including swiping, dragging, holding and tapping could be successfully detected.

Movie S8

The touch panel was cut using a scalpel then healed, and then used to write words and play games.

References

1 J. H. Yang, Z. K. Li and H. J. Zhu, *Appl. Catal. B*, 2017, **217**, 603-614.

2 C. Keplinger, J. Y. Sun, C. C. Foo, P. Rothemund, G. M. Whitesides and Z. G. Suo, *Science*, 2013, **341**, 984-987.

3 H. Haga, J. Yanase, Y. Kamon, K. Takatori, H. Asada and S. Kaneko, *SID Symp. Dig. Tec.*, 2010, **41**, 669-672.

4 H. Tian, Y. Yang, D. Xie, T. L. Ren, Y. Shu, C. J. Zhou, H. Sun, X. Liu and C. H. C. H. Zhang, *Nanoscale*, 2013, **5**, 890-894.

5 P. Salarizadeh, M. Javanbakht, S. Pourmahdian, M. S. A. Hazer, K. Hooshyari and M. B. Askari, *Int. J. Hydrog. Energy*, 2019, **44**, 3099-3114.